IEEE Access
Multidisciplinary | Rapid Review | Open Access Journal

Received July 15, 2018, accepted September 4, 2018, date of publication September 20, 2018, date of current version October 17, 2018.

Digital Object Identifier 10.1109/ACCESS.2018.2871060

Robust Joint Synchronization and Channel Estimation Approach for Frequency-Selective Environments

BRUNO LOPES[1], SÍLVIA CATARINO[1], NUNO M. B. SOUTO[1,3], (Senior Member, IEEE), RUI DINIS[2,3], (Senior Member, IEEE), AND FRANCISCO CERCAS[1,3], (Senior Member, IEEE)

[1]ISCTE-University Institute of Lisbon, 1649-026 Lisbon, Portugal
[2]FCT-UNL, 2829-516 Caparica, Portugal
[3]Instituto de Telecomunicações, 1049-001 Lisbon, Portugal

Corresponding author: Nuno M. B. Souto (nuno.souto@iscte.pt)

This work was supported by FCT-Fundação para a Ciência e Tecnologia and Instituto de Telecomunicações under Project UID/EEA/50008/2013.

ABSTRACT Supporting spontaneous low-latency machine-type communications requires fast synchronization and channel estimation at the receiver. The problems of synchronizing the received frame and estimating the channel coefficients are often addressed separately with the later one relying on accurate timing acquisition. While these conventional approaches can be adequate in flat fading environments, time dispersive channels can have a negative impact on both tasks and severely degrade the performance of the receiver. To circumvent this large degradation, in this paper, we consider the use of a sparse-based reconstruction approach for joint timing synchronization and channel estimation by formulating the problem in a form that is closely related to compressive sensing framework. Using modified versions of well-known sparse reconstruction techniques, which can take into account the additional signal structure in addition to sparsity, it is shown through numerical simulations that, even with short training sequences, excellent timing synchronization and channel estimation performance can be achieved, both in single user and multiuser scenarios.

INDEX TERMS Channel estimation, time synchronization, compressive sensing, sparse signal recovery.

I. INTRODUCTION

Fast and accurate timing synchronization is important to enable reliable communications in modern wireless systems and has a fundamental role within the context of extreme low-latency machine type communications [1]. Additionally, accurate channel estimation is crucial for enabling coherent data detection. Typically, both problems are handled separately, as in [2]–[5], and while reliable channel estimation methods depend on accurate timing acquisition, the latter is not guaranteed in time dispersive channels. Still, there have been a few attempts to address synchronization and channel estimation using a joint approach. Fechtel and Meyr [6] proposed algorithms for joint frame synchronization, frequency offset estimation and channel acquisition. One of the algorithms employed a data dependent approach and was capable of very good performance. However, its complexity grows exponentially with the length of the channel which limits its use to short time dispersions. Larsson *et al.* [7] presented a simple joint synchronization and channel estimation algorithm based on Maximum Likelihood (ML) estimation and Generalized Akaike Information Criterion information (GAIC). However, the proposed algorithm was designed specifically for the OFDM packet structure of the IEEE 801.11 WLAN standard. Zhang *et al.* [8] proposed an algorithm based on the shift delay characteristic of the synchronization sequence revealed in the channel estimation process. This was shown to reinforce the performance of fine timing synchronization and mean channel estimation error of OFDM systems.

Compressive sensing (CS) is a well-known signal processing paradigm that allows the efficient reconstruction of a signal with fewer samples than the Nyquist sampling theory requires, as long as it is sparse in a known transform domain [9], [10]. Several CS techniques have been proposed in the literature [11] with the greedy orthogonal matching pursuit (OMP) algorithm and ℓ_1-minimization being two of the most well-known approaches. Although ℓ_1-minimization enables good reconstruction performance,

it was shown in [12] that reweighting the ℓ_1 norm of the transformed object allows reducing the number of measurements needed for exact recovery of the original signal. CS has found a widespread adoption in many different fields with several applications already proposed for wireless communications [13]. One of the earliest and notable examples of CS adoption is within the context of channel estimation [14] which, amongst other advantages, can allow the reduction of the number of pilots required on multicarrier systems by exploiting the "delay-Doppler sparsity" [15]. A closely related problem which has not been so thoroughly addressed yet but which could also be dealt with CS techniques is in joint channel estimation and synchronization. Still, a method was recently proposed in [16] which exploits the sparsity of the equivalent channel vector. It is based on the direct application of OMP but assumes the transmission of training frames that are larger than data frames. Motivated by this, in this paper, we formulate the joint channel estimation and timing synchronization problem in a form that is closely related to CS framework. We then propose modified versions of sparse reconstruction techniques that allow the channel impulse response (CIR) to be obtained simultaneously to the symbol timing offset. These sparse methods are modified in order to handle the additional signal structure in the form of a bounded maximum distance between the positions of the first and last occurring nonzero elements. We also extend the proposed approach to underdetermined multiuser scenarios such as the ones that often arise in random access based networks where one spontaneous transmission can occur, originating from a set of several possible transmitters. Through numerical simulations we verify that the proposed schemes can achieve good performances both in terms of channel estimates and timing offset accuracy even when using short training sequences.

Notation: Matrices and vectors are denoted by uppercase and lowercase boldface letters, respectively. The superscripts $(\cdot)^{\mathrm{T}}$ and $(\cdot)^{\mathrm{H}}$ denote the transpose and conjugate transpose of a matrix/vector, $\|\cdot\|_p$ is the ℓ_p-norm of a vector, $\|\cdot\|_0$ is its cardinality, supp $(\mathbf{x})$ returns the set of indices of nonzero elements in $\mathbf{x}$ (i.e., the support of $\mathbf{x}$), diag $(\cdot)$ represents a diagonal matrix whose elements are contained in the argument vector, $\mathbf{I}_n$ is the $n \times n$ identity matrix and $\mathbf{1}$ is an all-ones column vector.

The remainder of the paper is organized as follows: section II introduces the signal model and formulates the joint synchronization and channel estimation problem. Section III presents several CS based algorithms adapted to the time synchronization and channel estimation tasks. Performance results obtained with these algorithms are then shown in section IV followed by the conclusions in section V.

II. SIGNAL MODEL AND PROBLEM FORMULATION

Let us assume that, for timing synchronization and channel estimation purposes, a training sequence $\mathbf{s} = \left[s_0\ s_1\ \cdots\ s_{N_c-1}\right]^T$ of length N_c is transmitted, followed by a guard period as shown in Fig. 1. The guard period has the purpose to help deal with the time dispersive nature of

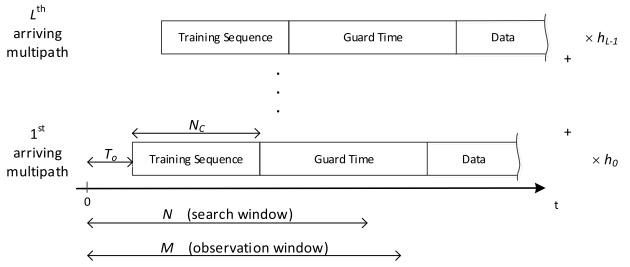

FIGURE 1. Frame structure and synchronization strategy.

the channel and can consist of either empty symbols or of a repetition of the initial part of the training sequence (which can alternatively be seen as a cyclic prefixed preamble). Although not addressed in this paper, the latter case can be useful for estimating and correcting the frequency offset in OFDM-based systems [2]. The signal is transmitted through the channel which is assumed to be represented by a finite impulse response filter $\mathbf{h} = [h_0\ h_1\ \cdots\ h_{L-1}]^T$, where $h_l \in \mathbb{C}$ and L is the maximum expected channel length, i.e. $\|\mathbf{h}\|_0 \leq L$. Note that not all h_l are necessarily nonzero and, in fact, the effective channel length (unknown at the receiver) can be much smaller than L. If the signal arrives at the receiver with an unknown delay of T_0 (in samples) then it can be written as the linear convolution of the delayed training sequence with the channel impulse response, i.e., as $y_t = \sum_{l=0}^{L-1} h_l s_{t-T_0-l} + n_t$, with $0 \leq t \leq M-1$. M is the number of observation samples and n_t represents noise. The received signal can be rewritten in a convenient form using matrix/vector notation as

$$\mathbf{y} = \mathbf{S}\mathbf{h}^{ext} + \mathbf{n}, \tag{1}$$

where $\mathbf{S}$ is an $M \times N$ Toeplitz matrix. For the case of empty guard periods (where $s_t = 0$ for $t < 0$ or $t > N_c - 1$), $\mathbf{S}$ is defined as

$$\mathbf{S} = \begin{bmatrix} s_0 & 0 & \cdots \\ \vdots & s_0 & \ddots \\ s_{N_c-1} & \vdots & \ddots \\ 0 & s_{N_c-1} & \\ \vdots & 0 & \ddots \\ & \vdots & \ddots \end{bmatrix}, \tag{2}$$

with N being the size of the search window (not necessarily equal to the size of the observation window M). Vector $\mathbf{h}^{ext}$ corresponds to the channel impulse response augmented with several zeros namely, T_0 zeros preceding the effective channel response followed by further $N-L-T_0$ zeros. This extended vector can be written as

$$\mathbf{h}^{ext} = \left[\underbrace{0\cdots0}_{T_0}\quad \mathbf{h}^T \quad \underbrace{0\cdots0}_{N-L-T_0}\right]^T. \tag{3}$$

The search window N can be defined around an initial coarse synchronization period flagged from some power measurement and threshold decision [6]. It can also be set according to the maximum expected propagation delay for a user, when a downlink control signal is present for timing uplink transmissions. It is important to note that the signal model just described is general in the sense that it can be applied to both single carrier and multicarrier systems, provided that they employ training blocks for estimation purposes.

Conventional approaches for accomplishing synchronization and channel estimation rely on performing both tasks separately. First, and assuming that the first channel tap is the strongest, an estimate of T_0 can be obtained using a simple cross-correlation based metric:

$$\hat{T}_0 = \underset{0\leq t\leq M-N_c}{\arg\max} \left|\mathbf{s}^H \mathbf{y}_{t:t+N_c-1}\right|^2. \tag{4}$$

After acquiring the timing of the first replica, the channel can be estimated using conventional least squares

$$\hat{\mathbf{h}} = \left(\bar{\mathbf{S}}^H \bar{\mathbf{S}}\right)^{-1} \bar{\mathbf{S}}^H \mathbf{y}_{\hat{T}_0:\hat{T}_0+N_c-1}, \tag{5}$$

where $\bar{\mathbf{S}} = \mathbf{S}_{\hat{T}_0:\hat{T}_0+N_c-1,\hat{T}_0:\hat{T}_0+L-1}$.

The conventional separate approach can be adequate for several scenarios, as long as the time dispersion caused by the channel is not large and the training sequence has near zero off-peak autocorrelation values (which often requires using long lengths). When these conditions are not satisfied, it can be seen from (4) that, even for time offsets that do not coincide with the beginning of a received replica, parts of other delayed replicas can be caught inside the correlation window. This will generate a nonzero result whose contribution is not only due to noise but also due to the nonzero correlations of the training sequence. The larger these correlation values, the higher the probability that the time offset maximizing (4) will be wrong, compromising also the subsequent channel estimation step. In order to improve the performance and attain higher reliability in a wider range of time dispersive scenarios, the synchronization and channel estimation problem should be addressed jointly and the prior information about the maximum expected channel length should be applied inside the process. Therefore, in the following we take this approach. Using signal representation (1) and integrating the prior information, the channel estimation and synchronization problem can be written as

$$\min_{\mathbf{h}^{ext}} f\left(\mathbf{h}^{ext}\right) \triangleq \left\|\mathbf{y} - \mathbf{S}\mathbf{h}^{ext}\right\|_2^2 \tag{6}$$

$$\text{subject to } \max\left\{|i-j+1| : h_i^{ext} \neq 0, h_j^{ext} \neq 0\right\} \leq L \tag{7}$$

which corresponds to a maximum *a posteriori* probability (MAP) estimator when the noise follows an uncorrelated zero-mean circularly symmetric Gaussian distribution. Assuming the typical scenario where the size of the search window N is large compared with L, or equivalently $\left\|\mathbf{h}^{ext}\right\|_0 \ll N$, it is possible to see that this formulation is closely related to sparse signal reconstruction problems and CS framework, since (7) restricts the cardinality of the solution $\mathbf{h}^{ext}$. However, this constraint is stronger than a simple cardinality one since it also imposes additional structure in the form of a bounded maximum distance between the positions of the first and last occurring nonzero elements.

III. JOINT TIMING AND CHANNEL ESTIMATION

Solving problem (6)-(7) directly requires an exhaustive search with combinatorial computational complexity. Therefore, alternative approaches that are computational feasible for problems of practical sizes must be used. Formulation (6)-(7) is related to cardinality constrained and minimization problems in CS framework. In fact, relaxing (7) into the simpler constraint

$$\left\|\mathbf{h}^{ext}\right\|_0 \leq L \tag{8}$$

allows the application of CS reconstruction techniques in order to recover $\mathbf{h}^{ext}$ and, indirectly, T_0 and $\mathbf{h}$. However, improved performance can be possible if the additional structure imposed by the exact constraint (7) is considered during the reconstruction process. In the following we propose several modified versions of sparse reconstruction techniques that can cope with problem (6)-(7).

Algorithm 1 Constrained Length OMP

1: **Input:** $\mathbf{y}$, $\mathbf{S}$, L, N
2: $\hat{\mathbf{h}}^{ext} = 0$, $\mathbf{r} = \mathbf{y}$, $\Omega = \emptyset$, $\Lambda = \emptyset$, $\hat{T}_0 = N-1$, $t_{\max} = 0$.
3: **for** $l = 0, 1, \ldots L-1$ **do**
4: $\quad\tilde{\mathbf{h}}^{ext} \leftarrow \mathbf{S}^H \mathbf{r}$.
5: $\quad$**repeat**
6: $\quad\quad t_{best} \leftarrow \underset{t\notin\Lambda}{\arg\max} \left|\tilde{h}_t^{ext}\right|$.
7: $\quad\quad \mathbf{\Lambda} \leftarrow \mathbf{\Lambda} \cup \{t_{best}\}$.
8: $\quad$**until** $t_{\max} - L + 1 \leq t_{best} \leq L - 1 + \hat{T}_0$
9: $\quad\mathbf{\Omega} \leftarrow \mathbf{\Omega} \cup \{t_{best}\}$.
10: $\quad\hat{\mathbf{h}}_{\Omega}^{ext} \leftarrow \left(\mathbf{S}_{\Omega}^H \mathbf{S}_{\Omega}\right)^{-1} \mathbf{S}_{\Omega}^H \mathbf{y}$.
11: $\quad\mathbf{r} \leftarrow \mathbf{y} - \mathbf{S}_{\Omega}\hat{\mathbf{h}}_{\Omega}^{ext}$.
12: $\quad t_{\max} \leftarrow \max(\Omega)$, $\hat{T}_0 \leftarrow \min(\Omega)$.
13: **end for**
14: $\hat{\mathbf{h}} \leftarrow \hat{\mathbf{h}}_{\hat{T}_0:\hat{T}_0+L-1}^{ext}$ (consider small magnitude elements as 0)
15: **Output:** $\hat{T}_0$, $\hat{\mathbf{h}}$.

A. CONSTRAINED LENGTH OMP

The first proposed approach follows a greedy strategy approximation and is based on the well-known OMP algorithm [10], which we modify in order to cope with the maximum channel length constraint (7). Algorithm 1 summarizes the main steps of the constrained length OMP (CL-OMP) method. In each iteration, the algorithm selects one new element for the support set Ω. Lines 5-8 and 12 represent the added modifications, which limit the addition of a new candidate position to the support of $\hat{\mathbf{h}}^{ext}$ if it will not result in the violation of (7). At line 10, the presented algorithm

adopts a conventional least squares (LS) approach for the computation of the channel estimates $\hat{\mathbf{h}}_{\Omega}^{ext}$ at the support positions (required for the residual **r**).In line 14, small magnitude elements of $\hat{\mathbf{h}}_{\hat{T}_0:\hat{T}_0+L-1}^{ext}$ are set to 0 using the following criterion which compares the magnitude of each candidate tap with the strongest one,

$$\hat{h}_{i-\hat{T}_0} = \begin{cases} \hat{h}_i^{ext}, & \left|\hat{h}_i^{ext}\right| \geq \eta \left\|\hat{\mathbf{h}}^{ext}\right\|_{\infty} \\ 0, & \left|\hat{h}_i^{ext}\right| < \eta \left\|\hat{\mathbf{h}}^{ext}\right\|_{\infty}, \end{cases} \tag{9}$$

where $\hat{T}_0 \leq i \leq \hat{T}_0 + L - 1$ and $\eta \geq 0$ (in the simulation results, we employed $\eta = 10^{-2}$).

B. REWEIGHTED ℓ_1-REGULARIZED OPTIMIZATION

The second approach for solving the reconstruction problem follows a strategy based on convex relaxation where the problem is replaced by a related ℓ_1 minimization problem, allowing the use of convex optimization techniques. Since these techniques often require the objective function to be analytic in its argument, they cannot be directly applied to real functions of complex variables like $f\left(\mathbf{h}^{ext}\right)$. In order to use these methods, the common approach is to convert the problem to the real domain by treating the real and imaginary parts of the optimization variables as independent ones. With this purpose, we rewrite (1) as

$$\widehat{\mathbf{y}} = \widehat{\mathbf{S}}\widehat{\mathbf{h}}^{ext} + \widehat{\mathbf{n}}, \tag{10}$$

with

$$\widehat{\mathbf{S}} = \begin{bmatrix} \mathrm{Re}\{\mathbf{S}\} & -\mathrm{Im}\{\mathbf{S}\} \\ \mathrm{Im}\{\mathbf{S}\} & \mathrm{Re}\{\mathbf{S}\} \end{bmatrix}, \quad \widehat{\mathbf{y}} = \begin{bmatrix} \mathrm{Re}\{\mathbf{y}\} \\ \mathrm{Im}\{\mathbf{y}\} \end{bmatrix},$$
$$\widehat{\mathbf{h}}^{ext} = \begin{bmatrix} \mathrm{Re}\left\{\mathbf{h}^{ext}\right\} \\ \mathrm{Im}\left\{\mathbf{h}^{ext}\right\} \end{bmatrix}, \quad \widehat{\mathbf{n}} = \begin{bmatrix} \mathrm{Re}\{\mathbf{n}\} \\ \mathrm{Im}\{\mathbf{n}\} \end{bmatrix}. \tag{11}$$

Note that while this representation increases the sizes of the matrices and vectors, the increase in the computation complexity is smaller than what one might expect, since all the operations become real-valued. We can then estimate $\widehat{\mathbf{h}}^{ext}$ by minimizing the Euclidean distance plus an ℓ_1-norm weighted regularization term (which is in fact related to the cardinality constraint of the problem)

$$\min_{\mathbf{h}_{ext}} \frac{1}{2}\left\|\widehat{\mathbf{y}} - \widehat{\mathbf{S}}\widehat{\mathbf{h}}^{ext}\right\|_2^2 + \lambda\left\|\mathbf{W}\widehat{\mathbf{h}}^{ext}\right\|_1 \tag{12}$$

where λ is a positive penalizing parameter and $\mathbf{W} = \mathrm{diag}\left(\begin{bmatrix} w_0 & \cdots & w_{2N-1} \end{bmatrix}\right)$ is a weighting matrix. These weights can be used for balancing the higher penalization imposed on larger coefficients of $\widehat{\mathbf{h}}^{ext}$ by the ℓ_1-norm, when compared to the ℓ_0-norm (cardinality). Adopting an approach similar to the one used in [19] for basis pursuit denoising (BPDN), we can rewrite (12) as

$$\min_{\mathbf{u},\mathbf{v}} \frac{1}{2}\left\|\widehat{\mathbf{y}} - \begin{bmatrix} \widehat{\mathbf{S}} & -\widehat{\mathbf{S}} \end{bmatrix}\begin{bmatrix} \mathbf{u} \\ \mathbf{v} \end{bmatrix}\right\|_2^2 + \lambda \mathbf{1}^T \begin{bmatrix} \mathbf{W} & 0 \\ 0 & \mathbf{W} \end{bmatrix}\begin{bmatrix} \mathbf{u} \\ \mathbf{v} \end{bmatrix} \tag{13}$$

$$\text{subject to } \mathbf{u} \geq 0, \quad \mathbf{v} \geq 0, \tag{14}$$

Algorithm 2 Constrained Length Reweighted ℓ_1-Regularized Optimization

1: **Input:** $\widehat{\mathbf{y}}$, $\widehat{\mathbf{S}}$, L, N,ε, Q
2: $\hat{\mathbf{h}}^{ext} = 0$, $\Omega = \emptyset$, $\hat{T}_0 = N - 1$, $t_{\max} = 0$
3: $w_i = 1$, $i = 0, \ldots, 2N - 1$.
4: **for** $q = 0, 1, \ldots Q - 1$**do**
5: Solve the quadratic problem (13)-(14) and obtain **u**, **v**.
6: $w_i = \frac{1}{u_i + v_i + \varepsilon}$, $i = 0, \ldots, 2N - 1$
7: **end for**
8: $\hat{\mathbf{h}}^{ext} \leftarrow \mathbf{u}_{0:N-1} - \mathbf{v}_{0:N-1} + \mathbf{i}\left(\mathbf{u}_{N:2N-1} - \mathbf{v}_{N:2N-1}\right)$
9: $\mathbf{\Lambda} \leftarrow \mathrm{supp}\left(\hat{\mathbf{h}}^{ext}\right)$ (consider small magnitude elements as 0)
10: **while** $\Lambda \neq \emptyset$ **and** $t_{\max} - \hat{T}_0 < L - 1$
11: $t_{best} \leftarrow \arg\max_{t \in \Lambda} \left|\hat{h}_t^{ext}\right|$
12: **if** $t_{\max} - L + 1 \leq t_{best} \leq L - 1 + \hat{T}_0$ **do** $\mathbf{\Omega} \leftarrow \mathbf{\Omega} \cup \{t_{best}\}$
13: $\mathbf{\Lambda} \leftarrow \mathbf{\Lambda} \backslash \{t_{best}\}$
14: $t_{\max} \leftarrow \max(\Omega)$, $\hat{T}_0 \leftarrow \min(\Omega)$.
15: **end while**
16: $\hat{\mathbf{h}} \leftarrow \hat{\mathbf{h}}^{ext}_{\hat{T}_0:\hat{T}_0+L-1}$ (consider small magnitude elements as 0)
17: **Output:** $\hat{T}_0$, $\hat{\mathbf{h}}$.

which is a convex quadratic program. Note that in this formulation $\widehat{\mathbf{h}}^{ext} = \mathbf{u} - \mathbf{v}$ and $\left|\widehat{h}_i^{ext}\right| = u_i + v_i$, with $i = 0, \ldots, 2N - 1$. Instead of simply solving (13)-(14) once with a fixed weighting matrix we can try to obtain improved performance through the use of an iterative reweighting procedure, following an idea similar to [12]. In this case, the weights in the diagonal of **W** are inversely proportional to the magnitude of the coefficients of $\widehat{\mathbf{h}}^{ext}$ (where $\left|\widehat{h}_i^{ext}\right| = u_i + v_i$) from the previous iteration plus a stabilizing parameter $\varepsilon > 0$ that avoids near zero divisors. This approach can successively improve the estimation of the nonzero positions by making the regularization term to better approximate the ℓ_0-norm. Algorithm 2 summarizes all the steps of the proposed constrained length reweighted ℓ_1-regularized (CL-IR-ℓ_1) approach. It consists in solving the quadratic problem (13)-(14) Q times using weights defined according to the solution of the previous iteration (line 6). Lines 10-15 are applied in order to force the solution to be feasible according to the maximum channel length constraint (7). If these lines are not used then the algorithm simply generates a generic sparse solution. In line 16, the same criterion defined in (9) can be applied to set the small magnitude elements of $\hat{\mathbf{h}}^{ext}_{\hat{T}_0:\hat{T}_0+L-1}$ as 0. Also note that when only one iteration is employed, i.e., $Q = 1$, then **W** is the identity matrix and the approach becomes closely related to BPDN [19]. We will refer to this special case as CL-BPDN. Regarding the penalizing parameter λ, [19] suggests the following choice

$$\lambda = \sigma\sqrt{2\log(N)}. \tag{15}$$

Problem (13)-(14), which is stated in line 5 of Algorithm 2, is a linear inequality constrained quadratic optimization problem. These types of problems can be efficiently addressed using a family of algorithms referred to in the literature as interior-point method (IPM) [17]–[19]. With these methods, the inequality constraints are encoded using a (self-concordant) logarithmic barrier function, which is subtracted from the objective function, in the case of the primal problem, and added to the objective, in the case of the dual problem. The goal is to obtain an approximate formulation of the original inequality constrained problem as an equality constrained one [18], [19]. Then, Newton's method can be directly used for solving the resulting modified Karush–Kuhn–Tucker (KKT) equations (i.e. the first order conditions for simultaneous optimality in the primal and dual barrier problems). In this case, a Newton step equation system is built and solved repeatedly using a varying barrier parameter until the algorithm converges to the required tolerances. There are several forms of interior-point algorithms, with the primal-dual interior-point methods often being more efficient due to the better than linear convergence [18].

C. ℓ_2-REGULARIZED OPTIMIZATION

While usually not employed for obtaining sparse solutions, the reconstruction problem can also be addressed through ℓ_2-norm regularization, as explained in [11], [19]. Using this approach, the problem can be formulated as

$$\min_{\mathbf{h}_{ext}} \ \left\|\mathbf{y}-\mathbf{S}\mathbf{h}^{ext}\right\|_2^2+\lambda\left\|\mathbf{h}^{ext}\right\|_2^2 \tag{16}$$

where the ℓ_1-norm regularization term has been replaced by and ℓ_2-norm term. It is easy to verify that this formulation has the following closed form solution

$$\hat{\mathbf{h}}^{ext}=\left(\mathbf{S}^H\mathbf{S}+\lambda\mathbf{I}_N\right)^{-1}\mathbf{S}^H\mathbf{y}. \tag{17}$$

Regarding the penalizing parameter λ, a value similar to the one used in BPDN, (15), can also be adopted [19]. To constrain the final estimate according to (7), the procedure matching lines 9 to 16 of Algorithm 2 can be directly applied which results in a constrained length ℓ_2-regularized algorithm (CL-ℓ_2).

D. POLISHING

After using an ℓ_1–based heuristic (CL-BPDN or CL-IR-ℓ_1) for obtaining an initial candidate solution for the original joint synchronization and channel estimation problem (6)-(7), a final polishing step can be applied in order to possibly find an improved candidate solution. This step is implemented using the initial candidate for fixing the sparsity pattern(support)and then computing the LS solution of the restricted problem. This procedure can be expressed as

$$\hat{\mathbf{h}}=\left(\hat{\mathbf{S}}^H\hat{\mathbf{S}}\right)^{-1}\hat{\mathbf{S}}^H\mathbf{y}, \tag{18}$$

where $\hat{\mathbf{S}}=\mathbf{S}_{:,\Lambda}$, i.e., it is a reduced system matrix comprising only the columns of $\mathbf{S}$ matching valid positions of the estimated support $\mathbf{\Lambda}=\text{supp}\left(\hat{\mathbf{h}}^{ext}\right)$. Note that this final step only improves the channel estimates, $\hat{\mathbf{h}}$.

E. EXTENSION TO MULTIUSER SCENARIOS

The proposed joint synchronization and channel estimation approach can be directly extended to multiuser scenarios such as those that arise in random access based networks. In these scenarios, a spontaneous transmission can occur originating from an unknown user within a set of N_u possible candidates. In this case, besides estimating the symbol timing offset and CIR, the receiver also has to detect the active user. To deal with the additional difficulty, we can adopt the following augmented definitions for $\mathbf{S}$ and $\mathbf{h}^{ext}$:

$$\mathbf{S}=\left[\mathbf{S}_0\cdots\mathbf{S}_{N_u-1}\right] \tag{19}$$

and

$$\mathbf{h}^{ext}=\left[\mathbf{h}_0^{ext^T}\cdots\mathbf{h}_{N_u-1}^{ext\ T}\right]^T. \tag{20}$$

Each $M\times N$ matrix $\mathbf{S}_u$ (with $u=0,\ldots,N_u-1$) follows the same structure as in (2), i.e., its columns comprise shifted versions of the u^{th} user specific training sequence. The $N\times 1$ vector $\mathbf{h}_u^{ext}$ represents the augmented channel impulse of user u which, can either be an all-zero vector if the user is inactive, or have the same structure defined in (3). Using these redefined matrices/vectors, the received signal can still be expressed as (1) and the recovery algorithms described previously can be applied directly. Note that since matrix $\mathbf{S}$ has a size of $M\times NN_u$ and the observation window has a maximum length of $N+N_c-1$, the scenario is usually underdetermined (i.e., $M<NN_u$). This extended model can also match a multiple input multiple output (MIMO) system with N_u transmitter antennas by simply making each user correspond to an antenna and having all the antennas active. In this case, there is no need to detect the active antennas as these are assumed to be known.

F. COMPLEXITY

In Table 1, we present the complexities in terms of real-valued floating-point operations (flops) of the proposed algorithms. To arrive at these expressions, we considered that complex valued sums count as 2 flops and complex valued multiplications count as 6 flops. We assume that in any of the methods, and as long as it is viable, all operations (multiplications, inverses, etc.) involving solely matrix S are precomputed. When precomputation is difficult to employ, as happens with CL-OMP due to the operation over a reduced system matrix dependent on an expanding estimated support, savings are still possible since only N_c consecutive elements are nonzero inside each column of $\mathbf{S}$. For CL-BPDN and CL-IR-ℓ_1 we assume the use of a general-purpose IPM as in [19] (Q_{IPM} is the number of iterations used inside the IPM), although it could be possible to derive a specifically tailored IPM that takes into account the special structure of $\mathbf{S}$ and save on the overall computational complexity.

TABLE 1. Number of real flops for different algorithms.

Detector	Complexity
Conventional (correlation+LS)	$(8N_c-2)NN_u+4L^3+L^2(4M+15)+L(12M-5)$
CL-OMP	$LNN_u(8N_c+1)+L^2(L+1)^2+\frac{1}{6}(4N_c+15)(2L^3+3L^2+L)$ $+\frac{1}{2}(18N_c+2M-5)(L^2+L)$
CL-λ_2	$(8M-2)NN_u+4L^3+L^2(4M+15)+L(12M-5)$
CL-BPDN	$\left[NN_u(48M+58+24N_c)\right.$ $\left.+8M^3+10M^2+M(32N_c^2-32N_c+15)-8N_c+8\right]Q_{IPM}$
CL-IR-λ_1	$6NN_uQ+Q\left[NN_u(48M+58+24N_c)\right.$ $\left.+8M^3+10M^2+M(32N_c^2-32N_c+15)-8N_c+8\right]Q_{IPM}$

IV. PERFORMANCE RESULTS

In this section, we evaluate the performance of the proposed approaches for joint synchronization and channel estimation. For the training sequences, we used Zadoff-Chu sequences [20] normalized as $|s_t| = 1$, for $0 \le t < N_c$. In most of the results, the observation window, M, used was $M = N + N_c - 1$ which is the minimum valid size without truncating the training sequence in the last taps. The maximum expected channel length is L=10. The initial delay T_0 of the first arriving multipath is randomly selected from the set $\{0, \ldots, N-L\}$ according to a uniform distribution. After the first multipath (which is always nonzero), each of the following L-1 positions in the channel impulse response $\mathbf{h}$ are selected as zero-valued with a probability of 0.5. Regarding the nonzero channel coefficients, these are chosen as independent and identically distributed, zero-mean, circularly symmetric, unit variance complex Gaussian random variables, i.e., $E[\|h_l\|^2] = 1/\|\mathbf{h}\|_0$ when $h_l \neq 0$ (for $0 \le l \le L$). The noise samples in $\mathbf{n} \in \mathbb{C}^{M\times 1}$, are independently selected according to a zero-mean circularly symmetric Gaussian distribution with covariance $2\sigma^2\mathbf{I}_M$. The channel estimation performance is evaluated in terms of normalized mean squared error (NMSE)

$$NMSE = E\left[\frac{\left\|\hat{\mathbf{h}}-\mathbf{h}\right\|_2^2}{\|\mathbf{h}\|_2^2}\right]. \tag{21}$$

The synchronization is evaluated through the timing error rate (TER) which is measured as the average number of incorrect positions in supp $\left(\hat{\mathbf{h}}^{ext}\right)$. The results are plotted as a function of the noise level $10\log_{10}\left(1/2\sigma^2\right)$. For all the algorithms, including the unmodified conventional ones, we applied the criterion defined in (9) for setting the small magnitude elements of $\hat{\mathbf{h}}^{ext}_{\hat{T}_0:\hat{T}_0+L-1}$ as 0.

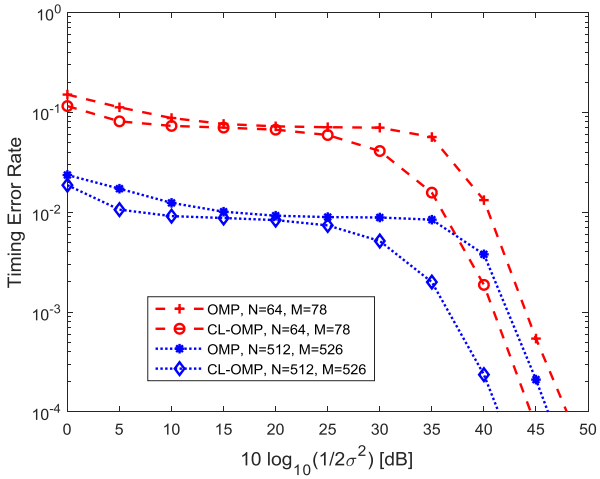

FIGURE 2. Timing error rate performance for OMP and CL-OMP ($N_c = 15$).

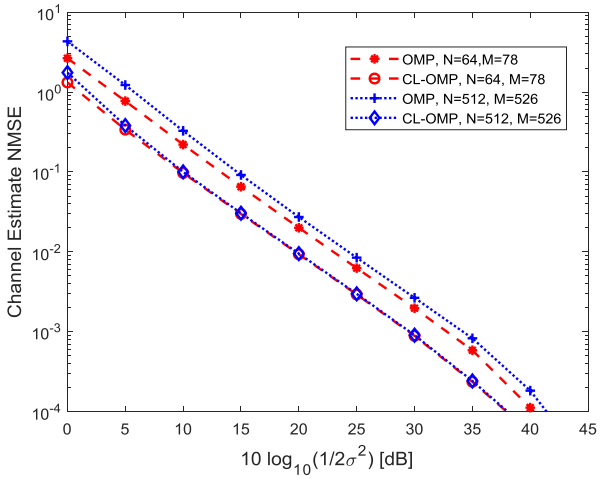

FIGURE 3. NMSE performance for OMP and CL-OMP ($N_c = 15$).

A. SINGLE USER

Considering only one known active user, Fig. 2 and 3 show the NMSE and TER performances of the conventional OMP and CL-OMP algorithms in two different scenarios: a small one, with $N = 64$ and $M = 78$, and a larger one, with $N = 512$ and $M = 526$. A short training sequence of length $N_c = 15$ was applied. It can be seen that the modification added to the OMP algorithm, which forces the solution to be feasible according to (7) instead of the conventional cardinality restriction (8), results in better performance both in terms of synchronization and channel estimation, achieving gains around 3 dB for the small scenario and 5 dB for the larger scenario. It is important to highlight that, for OMP, wrongly positioned taps can be spread quite far from the correct ones while for CL-OMP they will all be located close

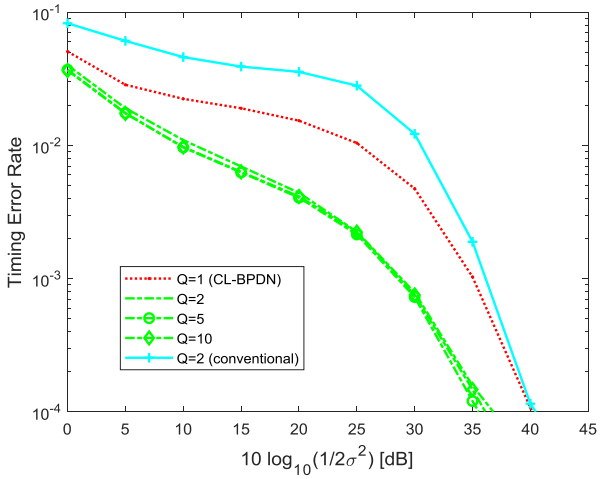

FIGURE 4. Timing error rate performance of CL-IR-ℓ_1 with different number of iterations ($N_c = 15$, $N = 128$ and $M = 142$).

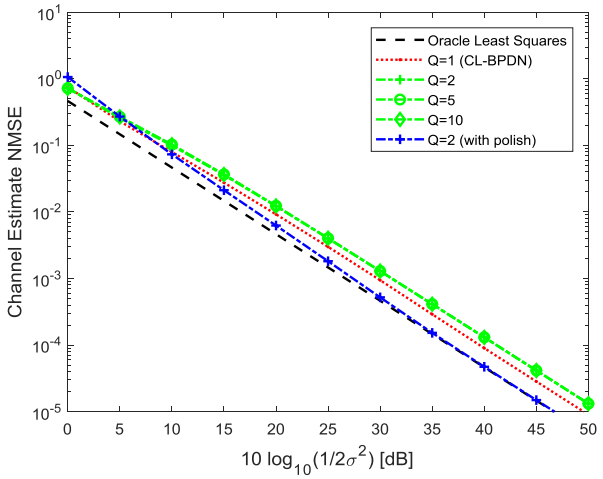

FIGURE 5. NMSE performance of CL-IR-ℓ_1 with different number of iterations ($N_c = 15$, $N = 128$ and $M = 142$).

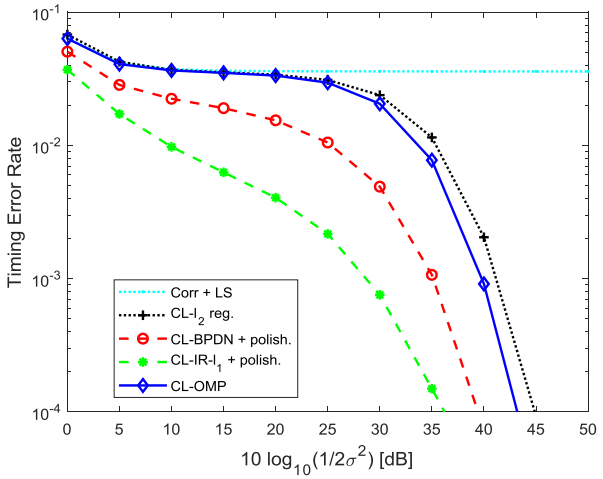

FIGURE 6. Timing error rate performance for different joint timing synchronization and channel estimation methods ($N_c = 15$, $N = 128$, $M = 142$).

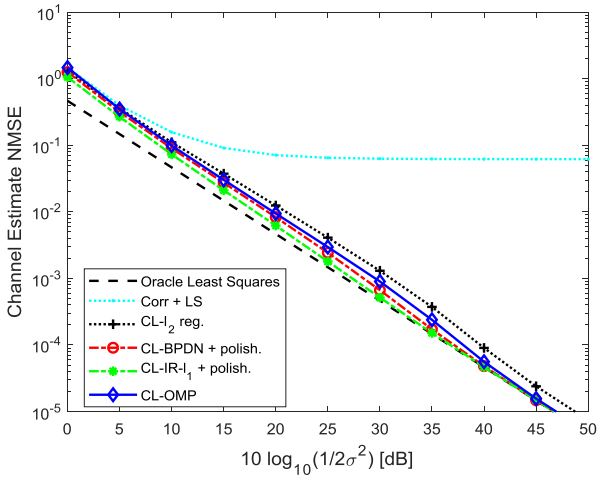

FIGURE 7. NMSE performance for different joint timing synchronization and channel estimation methods ($N_c = 15$, $N = 128$, $M = 142$).

to the real taps which reduces the negative impact on the time synchronization.

Fig. 4 and Fig. 5 illustrate the results obtained with the CL-IR-ℓ_1 method using different configurations, namely different number of iterations and the possible use of polishing. The scenario considered in this case was set as $N = 128$ and $M = 142$, with the same short training sequence of length $N_c = 15$. The curve with $Q = 1$ corresponds to the CL-BPDN, while the curve with 'conventional' label refers to a conventional reweighted ℓ_1 method whose generated solution is forced to satisfy the simpler cardinality constraint (8) only. Fig. 5 also includes an Oracle LS curve which represents an ideal case where the exact tap positions are known (i.e. perfect synchronization is assumed). It is visible that after only two iterations, the reweighted approach can result in substantial gains in terms of synchronization performance. After two iterations the improvements become small. The results also show a large gain of the modified CL-IR-ℓ_1 over the conventional method. Regarding the NMSE results, the CL-IR-ℓ_1 method suffers a small degradation compared to CL-BPDN. However, the degradation can be suppressed through the use of polishing, which results in a performance almost identical to the oracle LS for low noise levels.

Fig. 6 and Fig. 7 compare the performances of several synchronization and channel estimation methods also for the scenario with $N_c = 15$, $N = 128$ and $M = 142$. The 'Corr + LS' method corresponds to the conventional correlation approach (4) followed by LS estimation (5). For the CL-IR-ℓ_1 method, a total of $Q = 4$ iterations were applied. Regarding the synchronization results, CL-IR-ℓ_1 outperforms the other methods, while the correlation approach clearly has the worst behavior with a high irreducible TER floor. Although ℓ_2-norm based reconstruction tends to produce solutions which are not rigorously sparse, constraining the final estimate according to (7) allows the CL-ℓ_2 method

to achieve results in this scenario which are not far from CL-OMP. In terms of NMSE, the correlation approach has clearly the worst performance, having a high irreducible NMSE floor. Regarding the remaining methods, all have similar performances, with a small loss for CL-ℓ_2, and with CL-IR-ℓ_1 achieving the best results. For low noise levels, CL-OMP, CL-BPDN and CL-IR-ℓ_1 achieve performances nearly identical to the ideal Oracle Least Squares.

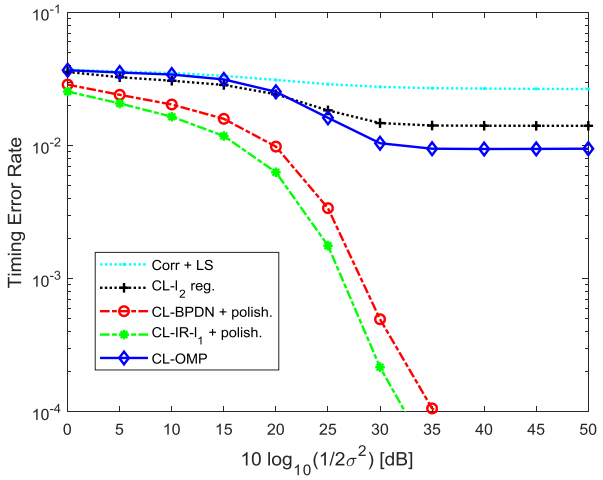

FIGURE 8. Timing error rate performance for an underdetermined scenario ($N_c = 127$ with a cyclic prefix length of 126, $N = 160$ and $M = 128$).

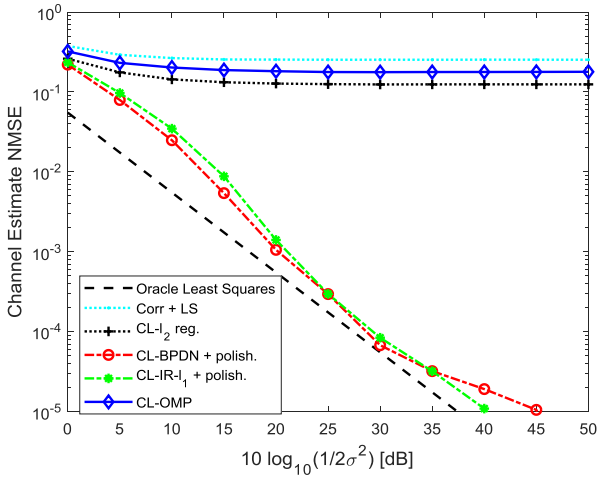

FIGURE 9. NMSE performance for an underdetermined scenario ($N_c = 127$ with a cyclic prefix length of 126, $N = 160$ and $M = 128$).

Fig. 8 and Fig. 9 illustrate the behaviour of all the methods in an underdetermined scenario where the observation window, M, is smaller than the search window N. In this case, we assume the transmission of a cyclic prefix consisting of the last $N_c - 1$ training symbols (which could represent a multicarrier transmission with repeated training blocks for accomplishing frequency offset correction [2]). The corresponding measurement matrix can be written as

$$\mathbf{S} = \begin{bmatrix} s_0 & s_{N_c-1} & & 0 & \\ \vdots & s_0 & & s_1 & \ddots \\ s_{N_c-1} & \vdots & \ddots & \vdots & \ddots \\ 0 & s_{N_c-1} & \ddots & s_{N_c-1} & \\ \vdots & 0 & \ddots & s_0 & \ddots \\ & \vdots & \ddots & \vdots & \ddots \\ & & & s_{N_c-1} & \\ & & & 0 & \ddots \\ & & & \vdots & \ddots \end{bmatrix}, \quad (22)$$

The scenario was configured as $N_c = 127$, $N = 160$ and $M = 128$. Looking at the results it can be seen that the performance of CL-ℓ_2 and CL-OMP clearly degrade and exhibit high irreducible error floors in the synchronization and channel estimation results. As for CL-BPDN and CL-IR-ℓ_1, despite the difficult underdetermined scenario, both methods are still capable of achieving very good performances.

B. MULTIPLE USERS

In this subsection we present performance results for a more difficult scenariowhere there is one uknown active user from a set of $N_u = 6$ possible transmitting candidates (the generalization to more than one unknown active users is straightforward). The search window has a length of $N = 80$ while the observation window is still $M = N + N_c - 1$.

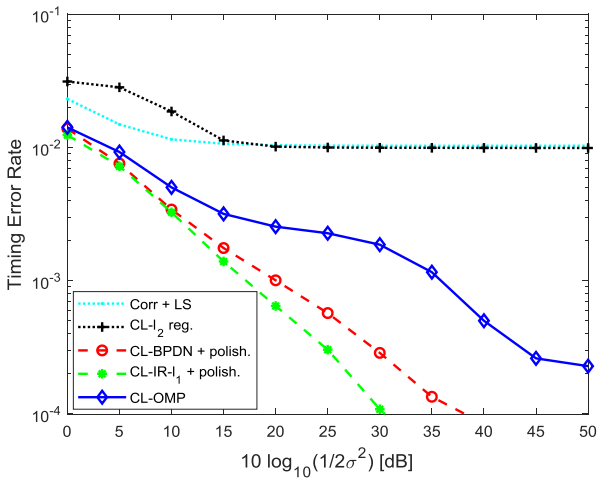

FIGURE 10. Timing error rate performance for an underdetermined scenario with 6 possible users ($N_c = 15$, $N = 80$, $N_u = 6$, $M = 94$).

Fig. 10 and Fig. 11 compare the TER and NMSE performances of the different methods when the training sequences have lengths of $N_c = 15$ which, clearly corresponds to an undetermined system (94 observations for estimating a vector with 480 elements). Similarly to what was observed in the previous results, the best performance is achieved by

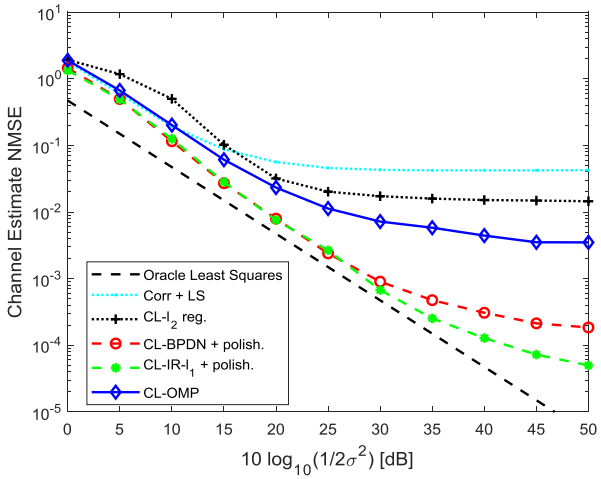

FIGURE 11. NMSE performance for an underdetermined scenario with 6 possible users ($N_c = 15$, $N = 80$, $N_u = 6$, $M = 94$).

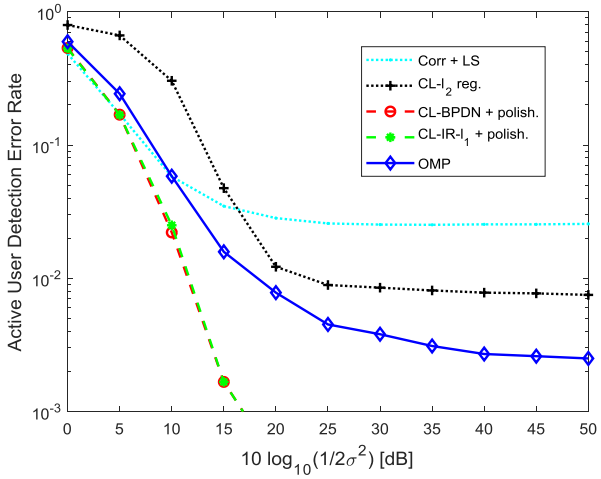

FIGURE 12. Active user detection error rate for an underdetermined scenario with 6 possible users ($N_c = 15$, $N = 80$, $N_u = 6$, $M = 94$).

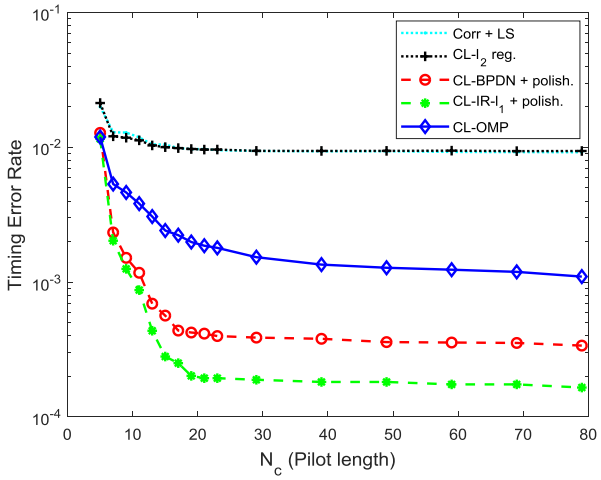

FIGURE 13. Timing error rate versus pilot length (N_c) in a multiuser scenario ($N = 80$, $N_u = 6$, $M = 79 + N_c$, $10\log_{10}\left(1/2\sigma^2\right) = 25$dB).

CL-IR-ℓ_1 and CL-BPDN, followed by CL-OMP and CL-ℓ_2. The correlation approach has the worst performance for low noise levels, where it exhibits high irreducible TER and

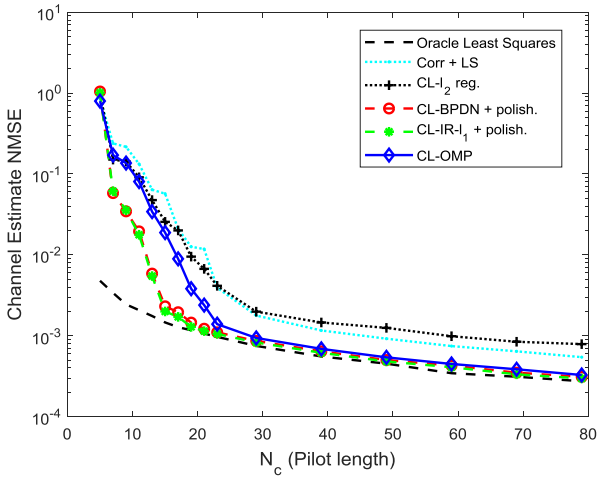

FIGURE 14. NMSE versus pilot length (N_c) in a multiuser scenario ($N = 80$, $N_u = 6$, $M = 79 + N_c$, $10\log_{10}\left(1/2\sigma^2\right) = 25$dB).

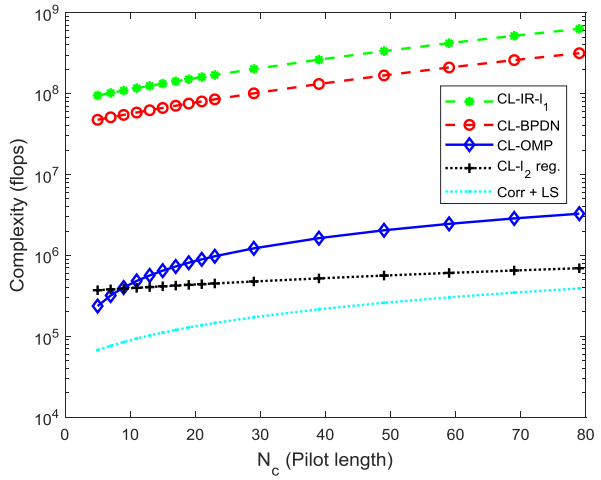

FIGURE 15. Complexity in flops versus pilot length (N_c) in a multiuser scenario ($N = 80$, $N_u = 6$, $M = 79 + N_c$).

NMSE floors. It is also interesting to look at the active user detection error rate (empirical probability of the active user being correctly detected) shown in Fig. 12. These results follow a trend similar to the TER and NMSE, with CL-IR-ℓ_1 and CL-BPDN clearly outperforming the other methods. In order to evaluate the impact of the training sequence length, Fig. 13 and Fig. 14 present the TER and NMSE as a function of N_c, for a fixed noise level of $10\log_{10}\left(1/2\sigma^2\right) = 25$dB. It can be seen that while longer training sequences benefit all the methods, sparse based reconstructions algorithms and in particular CL-IR-ℓ_1 and CL-BPDN, are able to maintain low TER and NMSE using shorter sequences than the conventional correlation approach. Looking at the corresponding computational complexity presented in Fig. 15, it is visible that the best performing methods, CL-IR-ℓ_1 and CL-BPDN, have the highest complexity cost. The conventional correlation approach has the lowest cost but, as previously seen, has the worst performance. The CL-OMP algorithm presents

itself as a good compromise between performance improvement and complexity cost.

V. CONCLUSIONS

In this paper we have addressed the problem of achieving fast time synchronization and channel estimation in frequency selective environments. To accomplish this, we formulated the channel estimation and synchronization problem in a form that is closely related to CS framework. We then applied modified versions of well-known sparse reconstruction techniques that, besides the sparsity, can also take into account the additional signal structure in the form of a bounded maximum distance between the positions of the first and last occurring nonzero elements. Simulation results confirmed that, even with short training sequences, excellent performance can be achieved, both in single user and multiuser scenarios, when compared with the conventional method based on time correlation and LS channel estimation.

REFERENCES

[1] M. Condoluci, M. Dohler, G. Araniti, A. Molinaro, and K. Zheng, "Toward 5G densenets: Architectural advances for effective machine-type communications over femtocells," *IEEE Commun. Mag.*, vol. 53, no. 1, pp. 134–141, Jan. 2015.

[2] T. M. Schmidl and D. C. Cox, "Robust frequency and timing synchronization for OFDM," *IEEE Trans. Commun.*, vol. 45, no. 12, pp. 1613–1621, Dec. 1997.

[3] M. M. U. Gul, X. Ma, and S. Lee, "Timing and frequency synchronization for OFDM downlink transmissions using Zadoff-Chu sequences," *IEEE Trans. Wireless Commun.*, vol. 14, no. 3, pp. 1716–1729, Mar. 2015.

[4] J. H. Manton, "Optimal training sequences and pilot tones for OFDM systems," *IEEE Commun. Lett.*, vol. 5, no. 4, pp. 151–153, Apr. 2001.

[5] M. K. Ozdemir and H. Arslan, "Channel estimation for wireless OFDM systems," *IEEE Commun. Surveys Tuts.*, vol. 9, no. 2, pp. 18–49, 2nd Quart., 2007.

[6] S. A. Fechtel and H. Meyr, "Fast-frame synchronization, frequency offset estimation and channel acquisition for spontaneous transmission over unknown frequency selective radio channels," in *Proc. PLMRC*, Yokohama, Japan, Sep. 1993, pp. 1–5.

[7] E. G. Larsson, G. Liu, J. Li, and G. B. Giannakis, "Joint symbol timing and channel estimation for OFDM based WLANs," *IEEE Commun. Lett.*, vol. 5, no. 8, pp. 325–327, Aug. 2001.

[8] Y. Zhang, J. Zhang, and M. Xia, "Joint timing synchronization and channel estimation for OFDM systems via MMSE criterion," in *Proc. Veh. Technol. Conf.*, Sep. 2008, pp. 1–4.

[9] D. L. Donoho, "Compressed sensing," *IEEE Trans. Inf. Theory*, vol. 52, no. 4, pp. 1289–1306, Apr. 2006.

[10] J. A. Tropp and A. C. Gilbert, "Signal recovery from random measurements via orthogonal matching pursuit," *IEEE Trans. Inf. Theory*, vol. 53, no. 12, pp. 4655–4666, Dec. 2007.

[11] Z. Zhang, Y. Xu, J. Yang, X. Li, and D. Zhang, "A survey of sparse representation: Algorithms and applications," *IEEE Access*, vol. 3, no. 1, pp. 490–530, May 2015.

[12] E. Candès, M. B. Wakin, and S. P. Boyd, "Enhancing sparsity by reweighted l_1 minimization," *J. Fourier Anal. Appl.*, vol. 14, nos. 5–6, pp. 877–905, Dec. 2008.

[13] J. W. Choi, B. Shim, Y. Ding, B. Rao, and D. I. Kim, "Compressed sensing for wireless communications: Useful tips and tricks," *IEEE Commun. Surveys Tuts.*, vol. 19, no. 3, pp. 1527–1550, 3rd Quart., 2017.

[14] C. R. Berger, Z. Wang, J. Huang, and S. Zhou, "Application of compressive sensing to sparse channel estimation," *IEEE Commun. Mag.*, vol. 48, no. 11, pp. 164–174, Nov. 2010.

[15] G. Taubock and F. Hlawatsch, "A compressed sensing technique for OFDM channel estimation in mobile environments: Exploiting channel sparsity for reducing pilots," in *Proc. IEEE Int. Conf. Acoust., Speech Signal Process.*, Mar. 2008, pp. 2885–2888.

[16] Ö. Özdemir, R. Hamila, N. Al-Dhahir, and I. Güvenç, "Sparsity-aware joint frame synchronization and channel estimation: Algorithm and USRP implementation," in *Proc. IEEE Mil. Commun. Conf. (MILCOM)*, Baltimore, MD, USA, Oct. 2017, pp. 647–652.

[17] J. A. Tropp and S. J. Wright, "Computational methods for sparse solution of linear inverse problems," *Proc. IEEE*, vol. 98, no. 6, pp. 948–958, Jun. 2010.

[18] S. Boyd and L. Vandenberghe, *Convex Optimization*. Cambridge, U.K.: Cambridge Univ. Press, 2004.

[19] S. S. Chen, D. L. Donoho, and M. A. Saunders, "Atomic decomposition by basis pursuit," *SIAM Rev.*, vol. 43, no. 1, pp. 129–159, 2001.

[20] D. C. Chu, "Polyphase codes with good periodic correlation properties (Corresp.)," *IEEE Trans. Inf. Theory*, vol. IT-18, pp. 531–532, Jul. 1972.

BRUNO LOPES received the B.Sc. and M.Sc. degrees in computer science and telecommunications from the ISCTE-Lisbon University Institute in 2015 and 2017, respectively. His research interests include wireless networks, coding, channel estimation, and synchronization.

SÍLVIA CATARINO received the B.Sc. degree from the ISCTE-Lisbon University Institute in 2015, where she is currently pursuing the M.Sc. degree in computer science and telecommunications. Her research interests include wireless networks, synchronization, channel estimation, and MIMO schemes.

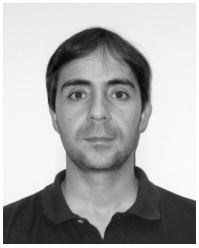

NUNO M. B. SOUTO (S'04–M'13–SM'16) graduated in aerospace engineering from the Avionics Branch, Instituto Superior Técnico, Lisbon, Portugal, in 2000. He received the Ph.D. degree in 2006. From 2000 to 2002, he was a Researcher in automatic speech recognition at the Instituto de Engenharia e Sistemas de Computadores, Lisbon. He joined the ISCTE-Lisbon University Institute as an Assistant Professor in 2006. He has been a Researcher at the Instituto de Telecomunicações, Portugal, since 2002, and has been involved in several international research projects and many national projects. His research interests include wireless networks, signal processing for communications, OFDM, single carrier transmission with frequency-domain equalization, channel coding, modulation, channel estimation, synchronization, MIMO schemes, wireless sensor networks, and unmanned aerial vehicles. He is a member of the IEEE Signal Processing Society.

RUI DINIS (S'96–M'00–SM'14) received the Ph.D. degree from the Instituto Superior Técnico (IST), Technical University of Lisbon, Portugal, in 2001, and the Habilitation degree in telecommunications from the Faculdade de Ciências e Tecnologia (FCT), Universidade Nova de Lisboa (UNL), in 2010. From 2001 to 2008, he was a Professor at IST. He is currently an Associate Professor at FCT-UNL. In 2003, he was an Invited Professor at Carleton University, Ottawa, ON, Canada.

He was a Researcher at the Centro de Análise e Processamento de Sinal, IST, from 1992 to 2005, and at the Instituto de Sistemas e Robótica from 2005 to 2008. Since 2009, he has been a Researcher at the Instituto de Telecomunicações. He has been actively involved in several national and international research projects in the broadband wireless communications area. His research interests include transmission, estimation, and detection techniques.

Dr. Dinis is an Editor of the IEEE TRANSACTIONS ON WIRELESS COMMUNICATIONS, the IEEE TRANSACTIONS ON COMMUNICATIONS (Transmission Systems—Frequency-Domain Processing and Equalization), and the IEEE TRANSACTIONS ON VEHICULAR TECHNOLOGY. He was also a Guest Editor of *Elsevier Physical Communication* (Special Issue on Broadband Single-Carrier Transmission Techniques).

FRANCISCO CERCAS (M'90–SM'15) received the Ph.D. degree from the Instituto Superior Técnico, Lisbon University, in 1996. He has more than 35 years of professional experience, including research and development at EID—Charneca da Caparica, Portugal, from 1982 to 1983, and 34 years of university teaching at Instituto Superior Técnico, Lisbon University, Portugal and ISCTE-University Institute of Lisbon since 1999, where he is currently a Full Professor and the President of the University Scientific Council. He was a Researcher at the Instituto de Engenharia de Sistemas e Computadores from 1984 to 1985, and at the Centro de Análise e Processamento de Sinal from 1986 to 1993. Since 1994, he has been a Researcher at the Instituto de Telecomunicações. He was also a Visiting Researcher at the University of Plymouth, U.K., from 1987 to 1992. He has participated in more than a dozen European Projects in the telecommunications area, namely, as the Portuguese Delegate in 4 COST actions (European Cooperation in Science & Technology). He has authored or co-authored a new class of codes, TCH (Tomlinson, Cercas, Hughes), and about 200 publications, including book chapters, journal, and conference papers. He holds one patent. His research interests include satellite and mobile communications, coding theory, spread spectrum communications, and related topics. He also supervised many Ph.D. and M.Sc. students.